Ping Wang
Zilin Chen
Hsueh-Chia Chang

Department of Chemical and
Biomolecular Engineering,
Center for Micro-fluidics
and Medical Diagnostics,
University of Notre Dame,
Notre Dame, IN, USA

Research Article

An integrated micropump and electrospray emitter system based on porous silica monoliths

The work presents the design of an integrated system consisting of a high-pressure electroosmotic (EO) micropump and a microporous monolithic emitter, which together generate a stable and robust electrospray. Both the micropump and electrospray emitter are fabricated using a sol–gel process. Upon application of an electric potential of sufficient amplitude ($>$2 kV), the pump delivers fluids with an electroosmotically induced high pressure ($>$1 atm). The same potential is also harnessed to electrostatically generate a stable electrospray at the porous emitter. Electrokinetic coupling between pump and spray produces spray features different from sprays pressurized by independent mechanical pumps. Four typical spray modes, each with different drop sizes and charge-to-mass ratios, are observed and have been characterized. Since the monolith is silica-based, this integrated device can be used for a variety of fluids, especially organic solvents, without the swelling and shrinking problems that are commonly encountered for polymer monoliths. The maximum pressure generated by a 100 μm id monolithic pump is ~3 atm at an applied voltage of 5 kV. The flow rate can be adjusted in the range of 100 nL/min to 1 μL/min by changing the voltage. For a given applied voltage across the pump and emitter system, it is seen that there exists one unique flow rate for which flow balance is achieved between the delivery of liquid to the emitter by the pump and the liquid ejection from the emitter. Under such a condition, a stable Taylor cone is obtained. The principles that lead to these results are also discussed.

Keywords: Electroosmotic pump / Electrospray / Silica monolith

1 Introduction

Recent years have witnessed many advances in micro-fabrication techniques and the development of micro-total analysis systems (μ-TAS) for chemical and biological analysis [1–3]. The miniaturization of analytical systems reduces the consumption of samples and allows assays to be performed rapidly and with less manual intervention. Different types of separations can be performed at the microscale, such as LC [4] and CE [5]. MS provides a means to rapidly and accurately identify the separands [6], and hence effective methods to couple the separation processes on microfluidic platforms to mass spectrometers are vital to the performance of μ-TAS systems. ESI, which utilizes a strong electric field to transfer ions from the solution to the gas phase, is currently the method for interfacing microfluidics to MS. When done directly from the fluidic outlets of microfluidic devices [7, 8], ESI results in the formation of large Taylor cones and large droplets, which are of limited use due to undesirably large dispersion and mixing. Various techniques have been adopted in order to generate smaller Taylor cones, and hence smaller droplets. Some researchers have used hydrophobic coatings on the surface of their microdevices or fabricated them using polymers with high hydrophobicity [9], while others have attached specially designed nozzles with narrow tips. These spray nozzles are fabricated by pulling or modifying conventional capillaries. However, the usefulness of the latter technique is limited for real-world solutions that often contain debris that can cause clogging.

Correspondence: Professor Hsueh-Chia Chang, Department of Chemical and Biomolecular Engineering, Center for Micro-fluidics and Medical Diagnostics, University of Notre Dame, Notre Dame, IN 46556, USA
E-mail: hchang@nd.edu
Fax: +1-574-631-8366

Abbreviations: DI, deionized; **EO**, electroosmotic

Monolithic emitters avoid this clogging problem because, as in filter beds, the multiplicity of flow paths ensure that some clear channels for the fluid remain even after a number of particles are trapped within the pores. Polymer monoliths [10–12] tend to suffer swelling and shrinking problems with typical organic solvents, although these problems can be reduced by increasing the degree of crosslinking. Silica monoliths do not have this drawback and hence, they should be a good matrix for electrospray emitters. They have been previously used for micro-LC (μ-LC) [13, 14], CEC [15], enzyme reactors and microflow-injection analysis (μ-FIA) [16–19]. They have been fabricated inside a capillary and are utilized as a spray emitter in this report. Besides resisting clogging, a relatively large inner diameter with sufficient mechanical stability allows it to sustain a high throughput. Silica monolithic capillaries can be manufactured with readily available materials without the need for laser-equipped capillary pullers. Modifying the sol–gel chemistry will enable the user to tailor its porosity and other physical properties.

Another important issue associated with ESI devices is the transport of liquid to the emitter. Such pumps must supply the desired amount of liquid for spraying at a high pressure ($\sim$1 atm) to overcome the large hydrodynamic resistance of the capillary, monolith and tip, as well as the capillary pressure due to surface tension at the meniscus at the emitter. Without pressurization and adequate fluid supply, the spray can be unstable. So far, embedded reliable micropumps are found in very few current-generation systems [20]. Instead, liquid transport is often accomplished through external devices such as syringe pumps or μ-LC pumps. The involvement of bulky peripheral apparatus significantly impairs the portability of microfluidic devices. Based on our earlier work [21], we propose an electro-osmotic (EO) micropump that meets these demands when properly integrated with the spray. The silica monolith used as an electro-osmotically active material for the pump is now used as a debris filter and a spray emitter matrix. The EO pump is connected to the electrospray emitter through a special Nafion junction so that both pumping and spraying can be accomplished on a single device. By controlling the pore size of the monolith, $\sim$3 atm pressure can be achieved to maintain robust sprays.

In this study, we demonstrate that the high-pressure EO pump can deliver liquids for electrospray with a flow rate ranging from 100 nL/min to 1 μL/min. The same electric voltage is used both to drive liquid through the micropump and to generate electrospray directly from the porous emitter. Due to the intricately coupled electrokinetics of the pump-spray device, the spray characteristics of this design are quite different from sprays pressurized by an independent mechanical pump. Depending on the

flow rate generated by the pump and the flow rate consumed by the electrospray, four different spray modes are observed. These modes are characterized visually and electrically. A simple hydrophobic surface modification is shown to reduce the spread of Taylor cones and dead volumes at the orifice due to wetting of the capillary surface. This study also provides the optimal conditions (the required voltage and flow rate) in the pump-spray unit to achieve stable spraying.

2 Materials and methods

2.1 Reagents and materials

Tetramethoxysilane (TMOS), urea and PEG (M_r 10 000) were obtained from Sigma-Aldrich and used without further purification. ACN and methanol (spectrum grade) were also purchased from Sigma-Aldrich. Sodium hydroxide, hydrochloric acid, acetone and acetic acid were purchased from Fisher Scientific. Novec™ hydrophobic coating EGC-1702 with a surface tension of 11 dynes/cm was obtained from 3 M and used to modify the surface of the capillary. All solutions were prepared using deionized (DI) water from a Milli-Q system (Millipore, MA). Fused-silica capillaries (100 μm id) were obtained from Polymicro Technologies (Phoenix, AZ). Prior to use, silica capillaries were pretreated using the same procedures as described in [18]. These pretreatments can eliminate impurities inside the capillary and activate the inside wall for further sol–gel reaction.

2.2 Formation of silica monoliths

The monolithic silica matrix was prepared by the procedures described in [16–19] with some modifications. Briefly, 0.5 mL of 0.01 M acetic acid, 54 mg PEG, 30 mg urea and 0.2 mL TMOS were mixed in a 1 mL size vial. The solution was stirred for about 40 min in an ice-water bath (0°C). The resultant homogeneous solution was injected into a 40 cm long capillary (100 μm id) using a syringe. The filled capillary was cured in an oven at 40°C for 24 h, subsequently treated for 3 h at 120°C with ammonia generated by the hydrolysis of urea and then washed with water and methanol. After drying, the temperature was increased from 40 to 300°C at a rate of 1°C/min, it was soaked for 4 h at 80, 120, 180 and 300°C, respectively, to effect decomposition of organic moieties in the capillary. Finally, the capillary was cooled down to room temperature at a rate of 1°C/min. This process was accomplished without serious deformation or fracture of the gel structure.
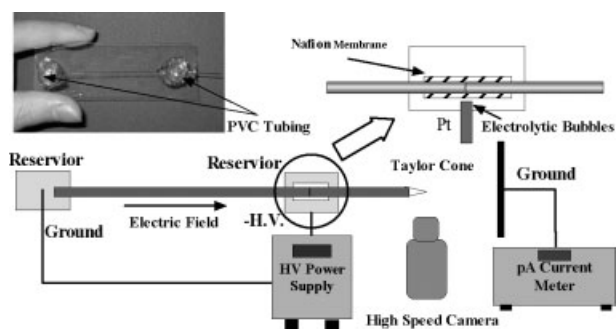
Figure 1. Schematic illustration of the assembled EO pump and the experimental setup for visual/electric characterization. The upper right part of this figure shows the configuration of the Nafion housing design. An image of assembled pump is shown on the upper left.

2.3 Device fabrication

Figure 1 shows a schematic illustration of the assembled kit. The monolithic capillary was mounted on a glass slide as shown in the upper left of the figure. A 6 cm long capillary with silica monoliths inside was connected to another 2 cm long identical capillary (filled with silica monoliths for electrospray characterization or unfilled for pump characterization only) *via* a Nafion® membrane tube (Perma Pure, NJ) with an id of 0.45 mm. A small amount of epoxy glue was applied inside and outside of the tube to minimize the dead volume and strengthen the connection as shown on the upper right of the figure. Two pieces of PVC tubing (5 mm id) were cut and glued to the two ends of the 6 cm long capillary and used as fluid reservoirs.

The ESI process was visually observed through an inverted microscope. The transient motion of Taylor cone was captured by a high speed camera (*i*-speed Olympus, USA). Total ion current generated from the spray between the tip and a copper plate electrode held at a distance of 1.5 cm away from the tip was measured using a pA meter (4140B, Hewlett-Packard). The oscillation of the ion current was recorded by a digital oscilloscope (TDS 2014, Tektronix). For each measurement, 1024 data points were acquired and transferred to a PC computer through an RS232 interface.

3 Results and discussion

3.1 Governing principles

The relationship between the flow rate Q_P and output pressure ΔP generated by a pump containing an electroosmotically active porous material is described by Eq. (1), which states that the sum of the properly scaled pressure and flow rate of the EO flow is always unity [21]

$$\frac{\Delta P}{\Delta P_{max}} + \frac{Q_P}{Q_{P_{max}}} = 1 \qquad (1)$$

where $Q_{P_{max}}$ is the maximum flow rate. For the monolithic pump, the maximum pressure ΔP_{max}, which is proportional to $1/a^2$ with a being the effective pore radius, can be measured experimentally.

The high hydrodynamic resistance offered by a small pore size is responsible for the high pressure. As a reference, it can be estimated that, for a 6 cm long open capillary with 100 μm id, the maximum EO pressure that can be generated using DI water with an electric field strength of 10^3 V/cm is only 1.677×10^{-3} atm or 170 Pa (zeta potential, $|\zeta| \sim 50$ mV). The capillary pressure of DI water for the same size capillary is about 1.441×10^{-3} atm or 146 Pa (surface tension ~ 73 dynes/cm at 20℃), which is almost comparable to the maximum EO pressure of the open capillary. Although an additional capillary aspiration force can be induced during electrospray, it is comparable in amplitude to the capillary pressure and is hence too weak to supply a steady flow rate for continuous spraying. Consequently, in order to generate a sufficiently high pressure to spray, a small pore size is essential for any upstream pump based on the EO phenomena, while a large cross-section area is desirable for a high liquid throughput. An optimum trade-off is then a bundle of parallel microchannels with a small pore size. Silica monolithic matrix offers such a structure with a small pore radius and multiple flow paths. Figure 2a compares the images of an empty capillary (on the right side) and a monolithic matrix (on the left side) using an optical microscope. Figures 2b–d show a cross-section image of the monolith using a scanning electron microscope. The diameter of the micropores can be estimated to be around 5 μm from Fig. 2d.

The flow rate produced by the device was determined by measuring the liquid out of an open capillary continuously in time and the pressure was calculated by pumping against compressed air. Three kinds of fluids, Tris–EDTA buffer solution (conductivity, $\sigma = 0.1$ S/m), stablized DI water ($\sigma = 10^{-4}$ S/m) and ACN ($\sigma < 10^{-6}$ S/m), were used as testing samples. As shown in Fig. 3, the maximum pressure and flow rate for DI water are 3 atm and 1 μL/min, respectively.

Electrolytic bubble generation is a common problem that plagues all systems like EO pumps when a direct current (DC) high voltage is applied. The use of Nafion tubing can minimize this effect. Since Nafion is a conductive polymer (*i.e.* a salt bridge) that permits transport of ions, it plays several important roles here. The conductive Nafion membrane allows electric current penetration to sustain electrolytic reaction on the cathode electrode, which is outside of the closed flow channel. The membrane also prevents flow leakage into the reservoir and hence maintains the
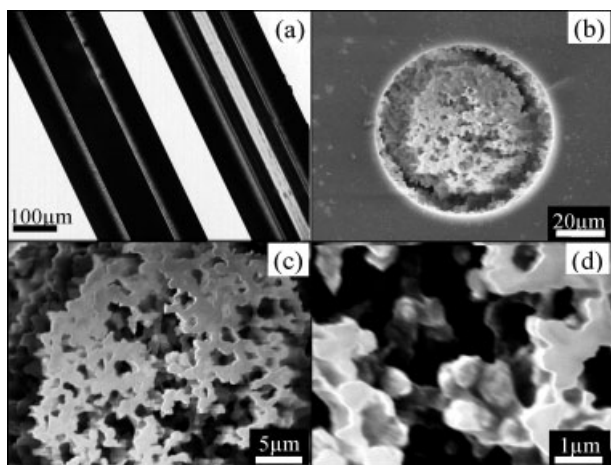
Figure 2. Photomicrographs and SEM images of silica monoliths fabricated inside 100 μm (id) capillaries. (a) Comparison between images of an empty capillary (on the right) and a monolithic capillary (on the left). (b–d) SEM images of the silica monolith at different magnifications.
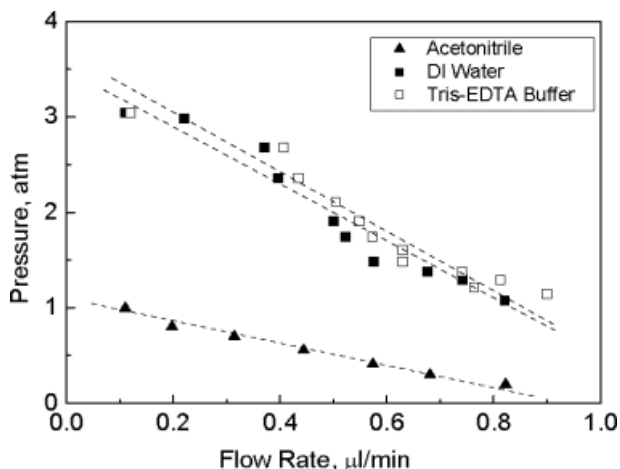
Figure 3. Measured output pressure of the EO pump as a function of liquid flow rate at an applied voltage of 5 kV. Tris–EDTA buffer (conductivity, $\sigma = 0.1$ S/m), DI water ($\sigma = 10^{-4}$ S/m) and ACN ($\sigma < 10^{-6}$ S/m) were used as working liquids.

hydrodynamic pressure created by the EO flow inside the capillary. The operating electric current in our experiment is very small $\sim$nA–μA so that concentration polarization near the Nafion surface can be neglected. As a result, gas bubble generation is not observed during the experiment even when electrolytes are used.

The spray flow rate plays an important role in determining the electrospray behavior. Once a downstream load, such as the spray emitter in our experiment, is connected to the pump, the flow rate is specified by the hydrodynamic resistance of the load. Equation (2) relates the external driving pressure, ΔP_d, and the flow rate Q_P for a porous capillary (the spray emitter)

$$\Delta P_d = \frac{8\eta l Q_P}{a^2 A_e} \tag{2}$$

where η is the viscosity of the fluid, l is the length of emitter capillary and A_e is the effective cross-sectional area of an capillary.

The output pressure at the end of the pump is the input pressure of the emitter and both pump and electrospray have the same flow rate. Therefore, by coupling Eqs. (1) and (2), a linear relation between electric field strength and liquid flow rate is obtained as shown in Eq. (3). Since the capillary pressure (1.441×10^{-3} atm) is much smaller than the pressure generated by the EO pump (>1 atm), we can neglect it and assume that the pressure head generated by the pump is entirely consumed by the emitter capillary. Equation (3) is the governing equation of the coupled EO/electrospray flow rate and indicates that the flow rate through the EO pump is reduced by a factor of $(1 + l/L)$ compared with an open capillary, L being the length of EO pump capillary, when a filled emitter capillary is connected

$$Q_P\left(1 + \frac{l}{L}\right) = -\frac{\varepsilon \zeta A_e}{\eta} E_z \tag{3}$$

where ε is the permittivity of the fluid and E_z is the electric field strength. Liquid flow rate with and without the emitter capillary are measured using ACN and DI water. To verify that our data are in agreement with Eq. (3), we scale the flow rate data without the emitter capillary by a factor of $((1 + l/L) \sim 1.333)$ and observe a good collapse in Fig. 4. As shown in the figure, the flow rate can be controlled from 100 nL/min to 1 μL/min by tuning the applied voltage which is the typical flow rate range for electrospray.
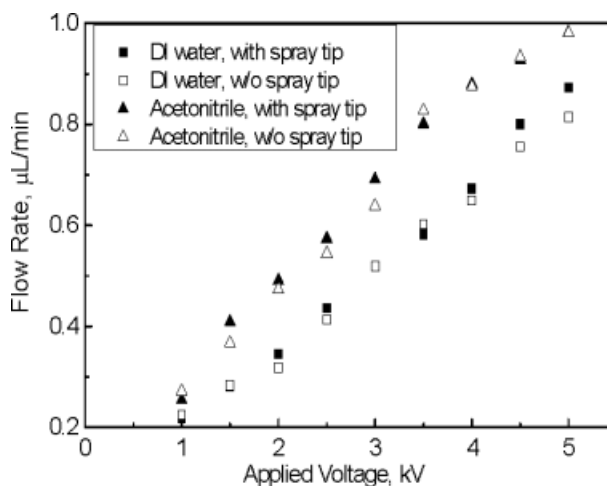
Figure 4. The measured flow rate as a function of applied voltage with and without a spray tip. The flow rate data of the EO pump without a spray tip is scaled by a factor of $(1 + l/L) = 1.33$. DI water and ACN are used as working liquids. Open symbols: without spray tip; filled symbols: with spray tip.

3.2 Electric and visual characterization

Since the current was carried by the charged droplets, the unstable electrospray with pulsating liquid meniscus resulted in an unstable spray current. Juraschek and Röllgen [22] have verified that there is an excellent correlation between the ion current oscillation in the mass spectrometer and the variations in the total spray current. One of the most important results of [22] is presented in their figure 20, which shows an excellent correlation between the ion current oscillation in the mass spectrometer and the variations in the total spray current. It is also known that specific spray modes can yield different distributions of droplet size and charge-to-mass ratio [23]. Small and monodisperse droplets having a high charge-to-mass ratio appear to offer analytical benefits, including improved ionization efficiencies and a reduced ion suppression. The most effective mode for producing such droplets is the cone-jet mode in which a stable, non-pulsating Taylor cone is formed.

The behaviour of the electrospray was observed under the microscope and the total ion current from the emitter exit simultaneously measured. ACN was used as the sample and sprayed directly towards a ground copper plate connected with a digital oscilloscope. The detailed electrospray process was monitored by high speed imaging at frame speeds ranging from 1000 to 10 000 frames/s. Figure 5 shows photomicrographs of four typical electrospray modes as observed. At low applied voltages, the droplet elongated and was deformed into an elliptically shaped cone. Beyond a threshold voltage (onset voltage of spray), the ellipsoid changed into a spindle shape as shown in Fig. 5a and the resulting electrospray also produced a jump in the ion current recorded at the ground copper plate. The current was measured by an oscilloscope and was found to be a periodic pulse with some noise. At this voltage, the electrospray consumed less liquid than that supplied by the EO pump. This flow imbalance generates drops that were polydisperse and subionized. When the voltage was increased further, the spindle spontaneously changed into a pointed Taylor cone and a steady current was measured as shown in Fig. 5b. The pulsation disappeared due to an exact balance between the supply of liquid to the emitter and ejection rate. A flat current was recorded by the oscilloscope even with a time resolution as high as 10^{-8} s. This constant current was a result of a stable ionic pathway established in the gas phase. This mode was the most effective one for producing monodispersed droplets and also had the highest ionization efficiency. As the applied voltage was increased further, the cone became unstable again with a decrease in cone size and jet breakup length as shown in Fig. 5c. This instability occurred presumably because the spray was emitting
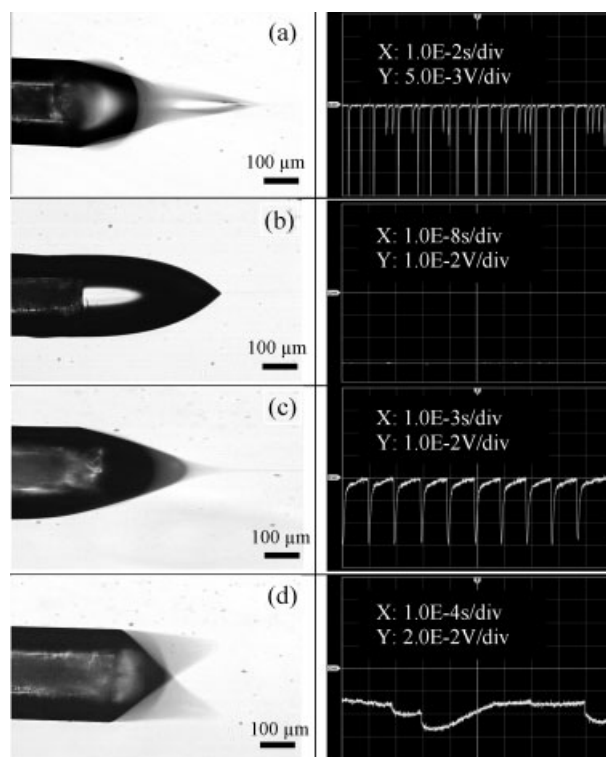
Figure 5. High-speed photomicrographs of drop ejection behavior for different applied voltage. The corresponding graphs on the right depict the electric current signals recorded by an oscilloscope connected to the ground electrode. (a) Spindle shape, (b) cone-jet shape, (c) pulsed cone shape, and (d) multiheaded cone shape. The applied voltages are −2.6, −3.1, −4.0 and −5.0 kV, respectively. The spacing between the spray tip to the counterelectrode is 1.5 cm. Scale bar: 100 μm.

more liquid than that supplied to it by the pump. The pulsation frequency was higher than that of the spindle mode. If the voltage was increased further, the single cone split into dual cones and these dual cones emanated from the emitter obliquely, as shown in Fig. 5d. In our setup, a threshold voltage of −2.2 kV was recorded for the onset of electrospray (Fig. 5a) with a 1.5 cm tip-to-counterelectrode spacing. The spray was observed to be stable for over 1 h when the appropriate voltage was set. Surprisingly, the threshold voltage had little dependence on the gap distance. Electrospray could still be observed even when all possible counterelectrodes were removed. We believe that it is due to the focusing shape of the electric field. The electric field lines are confined within the tip by the insulated capillary so that even when the counterelectrode is absent, the concentrated electric field can still sustain the electrospray.

As electrospray involves a transfer of charges between the electrospray emitter and the ground electrode, an electrospray current can be measured. It has been

reported [24] that the spray current and the applied electric field are related with the flow rate of spray Q_s by the equation

$$I_s \propto E^{3/7} Q_s^{4/7} \tag{4}$$

where I_s is the total spray electric current. This result is different from that of de la Mora and Loscertales's [25] highly conductive solutions ($>10^{-4}$ S/cm). Equation (4) indicates that the electrospray current increases with increasing electric field or applied voltage. In our particular setup, the liquid flow rate has a linear dependence upon the applied voltage as shown in Eq. (3) and Fig. 4. Therefore, Eq. (4) can be simplified to $I_s \propto E$ and $I_s \propto V$. This scaling argument hence predicts that the spray current increases linearly with the applied voltage.

The averaged spray current was measured by a pA meter for fabricated chip with a chip-to-counterelectrode spacing of 1.5 cm. This large spacing was chosen to ensure that the electric current passing through the oscilloscope was within its measurement limits. As shown in Fig. 6, a linear relationship is observed between I_s and V when the voltage is above 2 kV. Hence, the spray flow rate Q_s scales linearly with respect to voltage as the pump flow rate Q_p of Eq. (5), but with a different slope. The two flow rates intersect at the critical voltage of -3.1 kV when there is exact flow balance and a stable cone. Below that voltage, the liquid simply drips from the tip of the emitter instead of being sprayed and the resulting spray current is almost zero (<1 nA). Pulsation frequency of Taylor cone is also measured as a function of the applied voltage. The ejection frequency f for the unstable modes, can be estimated using the resonant frequency of a drop according to the Rayleigh dispersion relationship [26]

$$f = \frac{1}{2\pi} \sqrt{\frac{\gamma}{\rho R^3}} \tag{5}$$

where γ and ρ are the liquid surface tension and density, respectively, and R is the outer radius of the capillary. This estimated frequency is of 100–1000 Hz, in rough agreement with the measured frequency. As shown in Fig. 6, the frequency blows up (>100 MHz) at -3.1 kV when a stable Taylor cone (Fig. 5c) is formed. Below this critical voltage, large and polydispersed drops are ejected. Above it, the apex of the cone becomes unstable or even ramified. Both are not desirable for transferring ions from the solution to the MS detector. A small window near -3.1 kV produces stable cones due to flow balance and would yield optimum distributions of droplet size and charge-to-mass ratio, which are greatly beneficial for the whole ionization process.
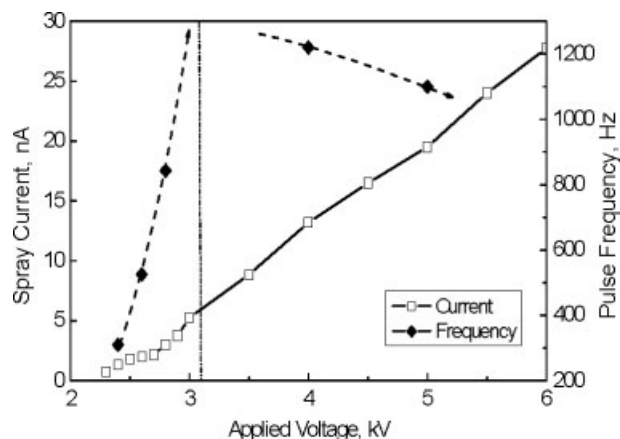
Figure 6. Measured electrospray electric current and the oscillation frequency as a function of the applied voltage (1.5 cm tip-to-counterelectrode spacing). A linear relationship can be observed between the spray current and the applied voltage. The oscillation frequency close to -3.1 kV is larger than 100 MHz and hence beyond our measurement limit, when a stable Taylor cone is established at the orifice of the emitter.
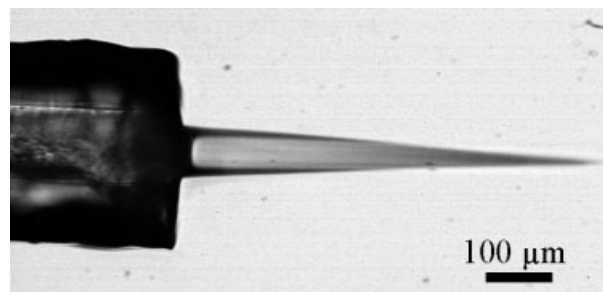
Figure 7. The spray jet at -3 kV after hydrophobic modification. The spacing between the spray tip to the counterelectrode is 1.5 cm. Scaled bar: 100 μm.

3.3 Hydrophobic modification of the spray emitter

The cone size is determined by the size of the wettable surface at the tip of the emitter. In our case, it is the outer diameter of the hydrophilic glass capillary, which is wetted by the liquid that forms into the Taylor cone. A large Taylor cone can cause unwanted dispersion and deteriorate upstream separation efforts. In order to reduce the dead volume, a hydrophobic coating (Novec electronic coating EGC-1702) was applied to render the capillary surface hydrophobic. The spray emitter was dipped into the solution, while air was pumped through the whole device simultaneously to prevent inflow into the capillary. After 10 s, the emitter was pulled out and dried in air. As shown in Fig. 7, instead of large Taylor cones, a threadlike liquid jet which has a diameter of the id of the capillary is observed at -3 kV with a tip-to-counterelectrode spacing of 1.5 cm. The liquid volume of

Taylor cone is reduced by a factor of $1 - (r/R)^2$, or ~90%, where r is the inner radius of the capillary. The ratio of the length and diameter of the jet is about 6. One possible explanation is that the electric polarization is confined to the liquid phase. If the liquid can only wet a smaller area after hydrophobic modification, the polarization becomes highly concentrated and introduces a stronger ejection force that can significantly deform the cone. Typically, the jet is found to be stable for more than 20 min. After that, the thin hydrophobic film gets partially damaged and a recoating process is necessary.

4 Concluding remarks

Silica-based monolithic structures have been synthesized inside a conventional capillary and used for pumping and electrospraying liquids. The silica-filled capillary developed in this study is very robust compared with a conventional needle-like capillary and can be manufactured with readily available materials in any laboratory. The multiple paths in the silica monoliths reduce clogging due to parallel channels. Due to the microscaled pore size inside the monolith, a pressure as high as 3 atm can be achieved. The same driving voltage is used simultaneously for the electrospray and to drive a high pressure EO pump to supply liquid to the spray. The intricate electrokinetic coupling between EO and electrospray has been characterized visually and electrically. The effects of flow rate, applied voltage, current magnitude on EO/electrospray behaviour follow expected theoretical trends. An optimal voltage is found to maintain a flow balance between EO pumping and electrospraying and to sustain a stable spray. A simple hydrophobic coating reduces the size (dead volume) of the Taylor cone. The above electrokinetic, hydrodynamic and ion current studies and characterization lay the necessary foundation for the design of a robust emitter for MS. Detailed MS measurements will be reported in a future paper.

5 References

[1] Burns, M. A., Johnson, B.N., Brahmasandra, S.N., Handique, K. *et al.*, *Science* 1998, *282*, 484–487.

[2] Harrison, D. J., Fluri, K., Seiler, K., Fan, Z. *et al.*, *Science* 1993, *261*, 895–897.

[3] Han, J., Craighead, H. G., *Science* 2000, *288*, 1026–1029.

[4] Abian, J., *J. Mass Spectrom.* 1999, *34*, 157–168.

[5] Khaledi, M. G., *High-Performance Capillary Electrophoresis: Theory, Techniques, and Applications*, Wiley-Interscience, New York 1998.

[6] Fenn, J. B., Mann, M., Meng, C. K., Wong, S. F., Whitehouse, C. M., *Science* 1989, *246*, 64–71.

[7] Xue, Q., Foret, F., Dunayevski, Y. M., Zavracky, P. M. *et al.*, *Anal. Chem.* 1997, *69*, 426–430.

[8] Ramsey, R. S., Ramsey, J. M., *Anal. Chem.* 1997, *69*, 1174–1178.

[9] Huikko, K., Östman, P., Grigoras, K., Tuomikoski, S. *et al.*, *Lab Chip* 2003, *2*, 67–72.

[10] Koerner, T., Turck, K., Brown, L., Oleschuk, R. D., *Anal. Chem.* 2004, *76*, 6456–6460.

[11] Shu, S., Lee, H., Douma, M., Koerner, T., Oleschuk, R. D., *Rapid Commun. Mass Spectrom.* 2005, *19*, 2671–2680.

[12] Koerner, T., Oleschuk, R. D., *Rapid Commun. Mass Spectrom.* 2005, *19*, 3279–3286.

[13] Lim, L. W., Uzu, H., Takeuchi, T., *J. Sep. Sci.* 2004, *27*, 1339–1344.

[14] Suzuki, A., Uzu, H., Masuoka, S., Li, X. *et al.*, *Bunseki Kagaku* 2004, *53*, 937–941.

[15] Tanaka, N., Kobayashi, H., Nakanishi, K., Minakuchi, H., Ishizuka, N., *Anal. Chem.* 2001, *73*, 420A–429A.

[16] Chen, Z., Hobo, T., *Anal. Chem.* 2001, *73*, 3348–3357.

[17] Z. Chen, K. Hayashi, Y. Ywasaki, R. Kurita, O. Niwa, K. Sunagawa, *Electroanalysis* 2005, *17*, 231–238.

[18] Chen, Z., Ozawa, H., Uchiyama, K., Hobo, T., *Electrophoresis* 2003, *24*, 2550–2558.

[19] Chen, Z., Wang, P., Chang, H.-C., *Anal. Bioanal. Chem.* 2005, *382*, 817.

[20] Laser, D. J., Santiago, J. G., *J. Micromech. Microeng.* 2004, *14*, 35–64.

[21] Wang, P., Chen, Z., Chang, H.-C., *Sens. Actuators B* 2006, *113*, 500–509.

[22] Juraschek, R., Röllgen, F. W., *Int. J. Mass Spectrom.* 1998, *177*, 1–15.

[23] Wei, J., Shui, W., Zhou, F., Lu, Y. *et al.*, *Mass Spectrom. Rev.* 2002, *21*, 148–162.

[24] Pfeifer, R. J., Hendricks, C. D., *AIAA J.* 1968, *6*, 496–502.

[25] de la Mora, J. F., Loscertales, I. G., *J. Fluid Mech.* 1994, *260*, 155–184.

[26] H. Lamb, *Hydrodynamics*, 6th edn., University Press, Cambridge Cambridge 1932.